Mater. Res. Soc. Symp. Proc. Vol. 841 © 2005 Materials Research Society R10.4.1/T6.4.1

Cross-Sectional TEM Studies of Indentation-Induced Phase Transformations in Si: Indenter Angle Effects

Songqing Wen[1], James Bentley[2], Jae-il Jang[1], and G.M. Pharr[1,2]
[1] The University of Tennessee, Dept. of Materials Science & Engr., Knoxville TN 37996
[2] Oak Ridge National Libratory, Metals & Ceramics Division, Oak Ridge TN 37831

ABSTRACT

Nanoindentations were made on a (100) single crystal Si wafer at room temperature with a series of triangular pyramidal indenters having centerline-to-face angles ranging from 35° to 85°. Indentations produced at high (80 mN) and low (10 mN) loads were examined in plan-view by scanning electron microscopy and in cross-section by transmission electron microscopy. Microstructural observations were correlated with the indentation load-displacement behavior. Cracking and extrusion are more prevalent for sharp indenters with small centerline-to-face angles, regardless of the load. At low loads, the transformed material is amorphous silicon for all indenter angles. For Berkovich indentations made at high-load, the transformed material is a nanocrystalline mix of Si-I and Si-III/Si-XII, as confirmed by selected area diffraction. Extrusion of material at high loads for the cube-corner indenter reduces the volume of transformed material remaining underneath the indenter, thereby eliminating the pop-out in the unloading curve.

INTRODUCTION

The generally recognized sequence for pressure-induced phase transformation of silicon as established in diamond anvil tests is that normal diamond cubic Si (Si-I) transforms to the metallic β-tin structure (Si-II) at a hydrostatic pressure of 11GPa, or at lower pressures when aided by shear stresses [1]. Upon decompression, the β-tin structure transforms to amorphous silicon (a-Si) at high release rates, or to a variety of metastable crystalline forms at low rates 1. Nanoindentation has also proven useful in the characterization of the pressure induced phase transformations of Si [2-14]. Since the hardness of Si is dominated by the pressure needed to induce the phase transformations, metastable phases are frequently observed within and around nanoindentation hardness impressions.

Indentation-induced phase transformations in Si have been studied mostly with spherical indenters and the Berkovich indenter - a triangular pyramid with a centerline-to-face angle of 65.3°. For these indenters, there is general agreement that the "elbow" observed in unloading curves at relatively low maximum loads is caused by the formation of amorphous silicon, whereas the "pop-out" observed at higher loads results from the nucleation and growth of metastable crystalline phases such as Si-III and Si-XII. Numerous studies have documented the post indentation structures of the deformed region of spherical, Vickers and Berkovich indentations using plan-view and cross-sectional TEM [5-13].

Recently, a systematic study by Jang et al. revealed that pop-out is absent when very sharp triangular pyramidal indenters are unloaded from high loads (figure 1a), even though the Raman spectra provide evidence for the existence of crystalline Si-III and Si-XII in the indent (figure 2) 14. This new finding led us to begin a detailed TEM study of the effects of indenter angle on the deformation structures of Si. Initial results of that study are reported here.

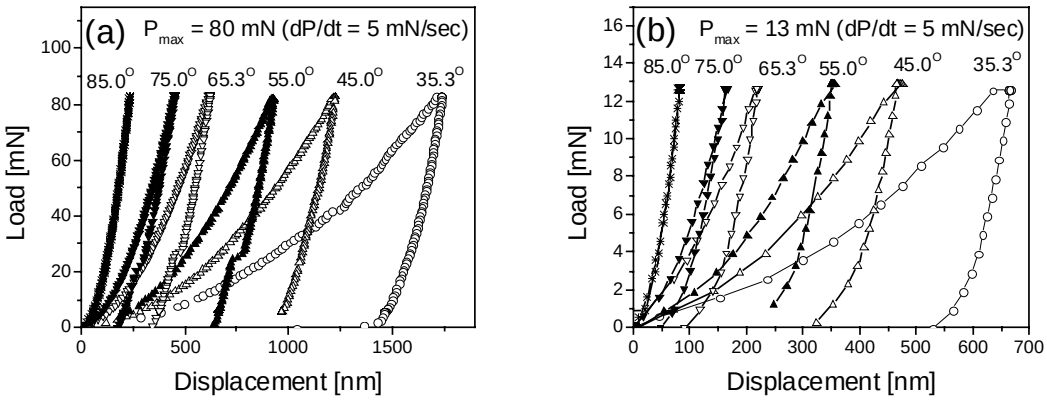

Figure 1. Load-displacement curves for nanoindentations made with triangular pyramidal diamonds with centerline-to-face angles varying from 35° to 85° at a constant loading/unloading rate of 5 mN/s: (a) P_{max} = 80 mN; (b) P_{max} = 13 mN [14].

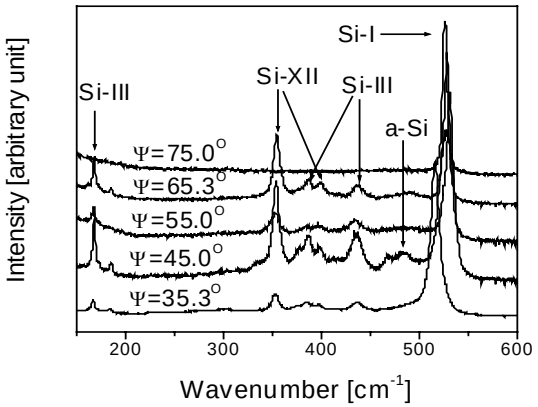

Figure 2. Raman spectra from nanoindents made with different indenters at P_{max} = 80 mN [14].

EXPERIMENTAL

Nanoindentation was conducted at the SHaRE User Center of the Oak Ridge National Laboratory using a Nanoindenter XP (MTS Systems, Oak Ridge TN). Undoped (100) single crystal Si wafer samples were indented at room temperature using a series of triangular pyramidal indenters with centerline-to-face angles of 35.3° (cube-corner), 45°, 55°, 65.3° (Berkovich), 75° and 85°. Two peak loads - 10 mN and 80 mN - were chosen to explore indenter angle effects at relative high and low loads. The loading/unloading rate was fixed at 5 mN/sec to eliminate complications brought about by rate effects. Cross-sections of the indentations were prepared utilizing a dual beam focused ion beam (FIB) mill. Cross-sectional transmission electron microscopy (TEM) and high resolution electron microscopy (HREM) were performed using FEI/Philips Tecnai20 and CM200FEG instruments at the SHaRE User Center. All the observations were made at 200kV.

RESULTS AND DISCUSSION

A. Indenter angle effects at low load

Figure 3 shows general SEM and TEM observations for indentations made at 10 mN with the 35°, 45°, 55°, and 65° indenters. Results for the 85° indenter are not included because it produced entirely elastic deformation (see figure 1). Cross-sections for the 75° indenter are currently in preparation. From the SEM plan views of the indentations, it is clear that residual depth increases as the indenter angle increases, in agreement with the indentation load-displacement curves (figure 1b). The surface radial cracking is most pronounced for the sharper indenters but is not present for indenter angles of 65° and above. The most notable feature is that the 35° cube-corner indenter shows not only the deepest hardness impression, but the transformed material also extrudes from underneath it to form a thin wispy layer on the surface. The cross-sectional TEM images reveal that the shape of the transformed zone is approximately the same for all indentations; however, the amount of transformed material in the zone decreases for the sharper indenters. For the Berkovich indenter (65°), the transformed material remains entirely beneath the indenter because the transformed zone does not extend beyond the edge of contact. The Berkovich indent shows no evidence of radial or median cracking, either in plan view or in cross-section. Cracks are observed for all other indenter angles, and material from the transformed zone flows into the median cracks. For the cube-corner indentation, the region of transformed material under the hardness impression is smaller than the others due to the extrusion of material to the surface.

Although the Berkovich indenter is frequently used for studies of this kind, indentations at low loads, e.g. 10 mN, have never been documented using cross-sectional TEM. The bright field image of a 10 mN Berkovich indent in figure 4a exhibits a large transformed zone (gray) with a few bright features, bend contours outside the transformed zone, and defects at the bottom of the indentation. Selected area diffraction (SAD) from the transformed zone (figure 4b) indicates

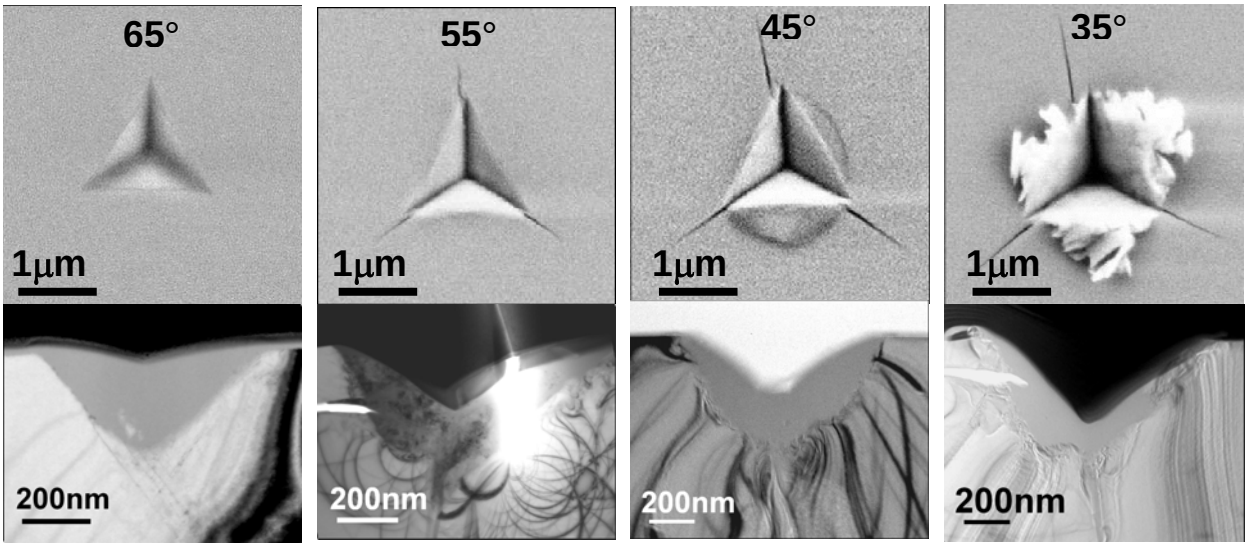

Figure 3. SEM plan-view and TEM cross-sectional images of low load indentations (10 mN) made with various triangular pyramidal indenters.

that material in the zone is mostly amorphous. The spot patterns in the SAD are produced by the surrounding untransformed Si-I matrix. There is dislocation activity underneath the transformed zone, which is further revealed by a dark field image (DF) taken with a Si-I (111) reflection (figure 4c). High resolution electron microscopy (HREM) was carried out at the crystalline-to-amorphous boundary and within the transformed zone (figure 5a). Microtwins were detected that are most extensive under the apex of the amorphous pocket and at the crystalline-to-amorphous boundary (figure 5b). Nanocrystalline grains of Si-I with typical dimensions between 5 and 20 nm are observed within the transformed region. However, observed crystallization of a-Si under the beam during HREM (figure 5c) gives rise to the concern that the original nanocrystals in the a-Si zone (figure 4a) might be artifacts caused by the ion beam during sample preparation. TEM examination of a low-load cube-corner indent is currently in progress.

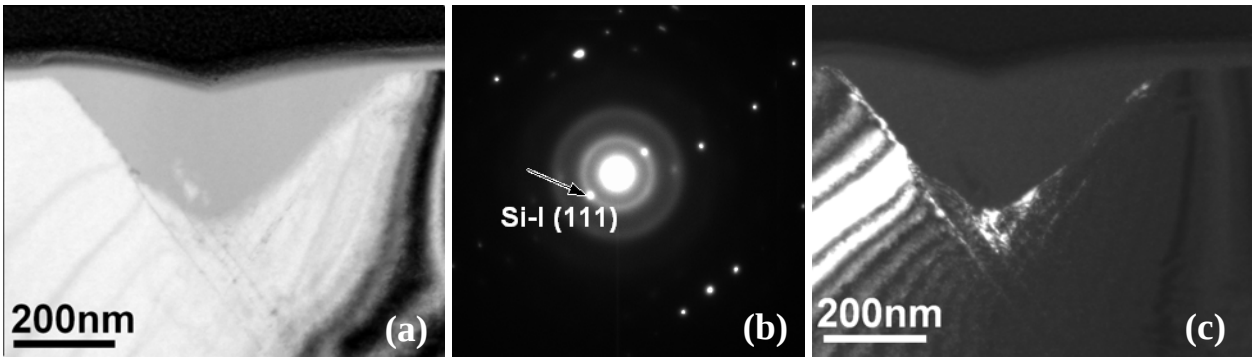

Figure 4. Cross-sectional TEM of a low load (10 mN) Berkovich indent: (a) bright field image; (b) SAD from the transformed zone; (c) dark field image from a Si-I (111) reflection.

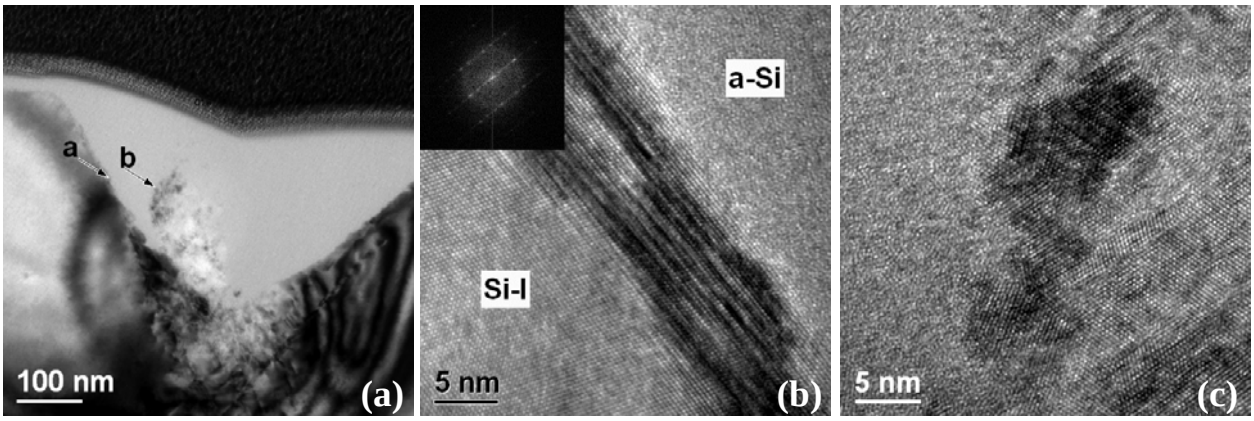

Figure 5. High resolution TEM of a low-load (10 mN) Berkovich indent: (a) bright field TEM image; (b) microtwins at the crystalline-to-amorphous boundary; (c) crystallization in the amorphous transformed zone induced by the electron beam.

B. Indenter angle effects at high load

Unlike the low-load condition, both the high-load Berkovich and cube-corner indentations made at 80 mN show radial cracks, lateral cracks, and median cracks (figure 6). The Berkovich indentation exhibits a well-capped transformed zone that is generally nanocrystalline in nature (figure 6b). The structure was confirmed by SAD to be mixture of crystalline Si-I, Si-III/Si-XII, which is in good agreement with Raman data (figure 2) and other microscopy results [9-13]. In contrast, the high-load cube-corner indentation shows extensive extrusion of the transformed material and very little remaining under the hardness impression. Since it is the volume change during phase transformation that gives rise to the pop-out event during unloading, the extrusion explains the absence of the pop-out event for the cube-corner indenter. This is a common feature for the 35° indenter and is occasionally observed for 45° indentations as well. It is noted that the appearance of the extruded material again strongly indicates the ductile and metallic-like nature of the transformed material under pressure.

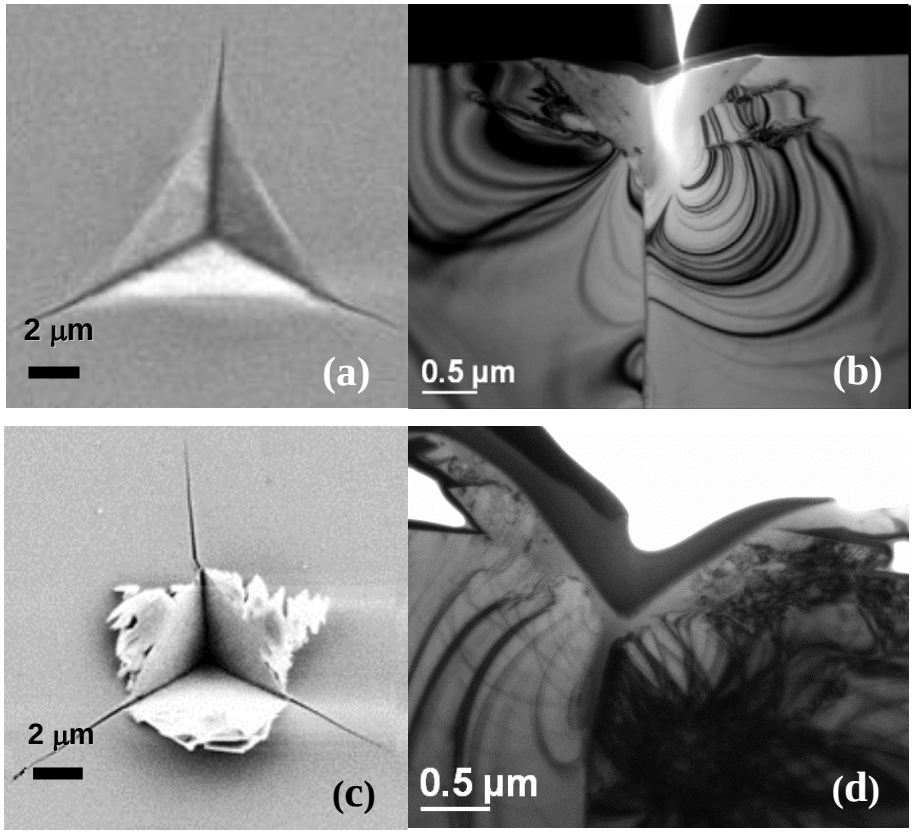

Figure 6. SEM plan-view and TEM cross-sectional images of high load indentations (80 mN): (a) and (b) Berkovich indentation; (c) and (d) cube-corner indentation.

CONCLUSIONS

Cross-sectional TEM and plan-view SEM observations show that cracking and extrusion in (100) Si are more prevalent for indenters with sharp centerline-to-face angles. At low loads (10 mN), the transformed material is confirmed to be amorphous Si for all indenter angles. Cracking is not observed when indenting with the Berkovich indenter at low loads, but at high loads (80 mN), cracking is observed for all indenters with angles in the range 35°-65°. Selected area diffraction confirms that the transformed material remaining underneath the high-load Berkovich indents is a nanocrystalline mixture of Si-I and Si-III/Si-XII. Extrusion of transformed material into the median cracks is a common feature for all indenters. Cross-sectional TEM explains the absence of pop-out for cube-corner indenters. Specifically, because the transformed zone extends beyond the edge of contact, there is extensive extrusion of transformed material and little remains under the hardness impression to reverse transform during unloading.

ACKNOWLEDGEMENTS

This research was sponsored by the National Science Foundation under grant number DMR-0203552, and by the Division of Materials Sciences and Engineering (SHaRE User Center), U. S. Department of Energy, under Contract DE-AC05-00OR22725 with UT-Battelle, LLC. The authors would like to thank Dr. Ting Tsui at Texas Instruments for the cross-sectional TEM specimen preparation, and Dr. Michael Lance for micro-Raman phase characterization.

REFERENCES

1. J.Z. Hu, L.D. Merkle, C.S. Menoni, and I.L. Spain, Phys. Rev. **B34**, 4679 (1986).
2. G.M. Pharr, W.C. Oliver, and D.S. Harding, J. Mater. Res. **6**, 1129 (1991).
3. G.M. Pharr, W.C. Oliver, R.F. Cook, P.D. Kirchner, M.C. Kroll, T.R. Dinger, and D.R. Clarke, J. Mater. Res.**7**, 961 (1992).
4. V. Domnich and Y. Gogotsi, Rev. Adv. Mater. Sci. **3**, 1 (2002).
5. D. L. Callahan and J. C. Morris, J. Mater. Res. **7,** 1614 (1992).
6. T.F. Page, W.C. Oliver, and C.J. McHargue, J. Mater. Res. **7,** 2431 (1992).
7. Y.Q. Wu, X.Y. Yang, Y. B. Xu, Acta Mater. **47**, 2431 (1999); J. Mater. Res. **14,** 682 (1999).
8. A.B. Mann, D. van Heerden, J.B. Pethica, P. Bowes, and T.P. Weihs, J. Mater. Res. **15,** 1754 (2000).
9. S.J. Lloyd., J.M. Molana-Aldareguia, and W.J. Clegg, J. Mater. Res. **16,** 3347 (2001).
10. J.E. Bradby, J.S. Williams, J. Wong-Leung, M.V. Swain, and P. Munroe, Appl. Phys. Lett. **77**, 3749 (2000); J. Mater. Res. **16**, 1500 (2001).
11. H. Saka, A.S. Himatani, M. Suganuma, and Suprija, Phil. Mag. **A82**, 1971 (2002).
12. D.B. Ge, V. Domnich, and Y. Gogotsi, J. Appl. Phys. **93**, 2418 (2003).
13. I. Zarudi and L.C. Zhang, Appl. Phys. Lett. **82**, 874 (2003); J. Mater. Res. **19**, 332 (2004).
14. J-I. Jang, M.J. Lance, S.Q. Wen, T.Y. Tsui, and G.M. Pharr, Acta Mater. (in press)